Quantum modulation of the Kondo resonance of Co adatoms on Cu/Co/Cu(100)

Takashi Uchihashi,^{1,2,*} Jianwei Zhang,¹ Jörg Kröger,¹ and Richard Berndt¹

¹Institut für Experimentelle und Angewandte Physik,

Christian-Albrechts-Universität zu Kiel, D-24098 Kiel, Germany

²Nano System Functionality Center, National Institute for Materials Science, Tsukuba 305-0044, Japan

(Dated: May 9, 2022)

Low-temperature scanning tunneling spectroscopy reveals that the Kondo temperature $T_{\rm K}$ of Co atoms adsorbed on Cu/Co/Cu(100) multilayers varies between 60 K and 134 K as the Cu film thickness decreases from 20 to 5 atomic layers. The observed change of $T_{\rm K}$ is attributed to a variation of the density of states at the Fermi level $\rho_{\rm F}$ induced by quantum well states confined to the Cu film. A model calculation based on the quantum oscillations of $\rho_{\rm F}$ at the belly and the neck of the Cu Fermi surface reproduces most of the features in the measured variation of $T_{\rm K}$.

PACS numbers: 68.37.Ef,72.10.Fk,73.21.-b,73.63.-b

Magnetic atoms interacting with their environment are fundamentally important in extensive fields of modern physics. Among all, the Kondo effect, a representative phenomenon resulting from the exchange interaction of a local spin with surrounding conduction electrons, is observed below a characteristic Kondo temperature $T_{\rm K}$. One of its hallmarks is the Kondo resonance whose width is given by k_BT_K (k_B : Boltzmann's constant). The Kondo resonance may be directly investigated using low-temperature scanning tunneling microscopy $(STM)^{2,3,4}$ or various quantum dots.^{5,6,7} Furthermore, artificial modification of the Kondo effect was investigated using atom manipulation^{8,9,10} and controlled tip contact.¹¹ More recently, a molecular Kondo effect has been investigated.^{12,13,14,15} Apart from the Kondo effect, the recent advancement of the spintronics has raised a strong interest in spin manipulation and in tailoring exchange interaction at atomic scale. 16,17 The observation of spin-related phenomena using low temperature STM and their control with artificial nanostructures are crucial for realizing such promises.

Here we use a model system for tuning the singleadatom Kondo temperature by means of variations of the local density of states at the Fermi level. In particular, single Co atoms are adsorbed on multilayers of Cu and Co grown on a Cu(100) surface and modifications of the Kondo resonance are measured as a function of the Cu layer thickness. Scanning tunneling spectroscopy is used to identify quantum well (QW) states of the Cu film. The absolute thickness of Cu overlayers, d_{Cu} , is locally determined from characteristic QW state energies. The Kondo temperature determined from spectra of the differential conductance (dI/dV) taken on single Co adatoms varies between 60 K and 134 K with decreasing Cu coverage from 20 to 5 atomic layers. Much of this variation is reproduced by a model calculation based on the quantum oscillations at the belly and the neck of the Cu Fermi surface. The phases of these oscillations are found to deviate from a theoretical prediction for Cu/Co/Cu(100) multilayers, suggesting the effect of Co adatoms on the phase shift at the Cu/vacuum interface.

The experiments were performed with a home-built

low temperature STM operated at 7K and in ultrahigh vacuum with a base pressure of 10^{-9} Pa. Samples and W tips were prepared by annealing and argon ion bombardment. Crystalline order was checked by lowenergy electron diffraction (LEED) while preliminary estimates of Co and Cu film thicknesses were performed by Auger electron spectroscopy (AES). Spectra of dI/dVwere acquired by standard lock-in detection. The clean Cu(100) surface was covered at room temperature (RT) with 10 ML of Co using an electron beam evaporator and an evaporant of 99.99 % purity. We define a monolayer (ML) as one Co atom per Cu atom. Subsequently, Cu was deposited at RT on the Co surface from a copper wire of $99.995\,\%$ purity wrapped around a tungsten filament. High deposition rates of $\approx 6 \,\mathrm{ML\,min^{-1}}$ were necessary to suppress heating from the filament and concomitant intermixing of Cu and Co. 18 Co atoms were deposited on the cold surface by electron beam evaporation.

We adopted a Cu/Co/Cu(100) system as a substrate for tuning the Kondo effect because extensive studies on this multilayer system are available. 19 An excellent lattice matching enables epitaxial growth of a face-centered cubic Co(100) layer on Cu(100), rather than a bulk-like hexagonal close-packed Co layer, and a subsequent epitaxial growth of Cu(100) on Co(100) (Fig. 1(a)). Figure 1(b) presents a constant-current STM image of Cu(100) with a Co coverage of 10 ML which reveals layer-by-layer epitaxial growth of Co. A subsequently deposited Cu layer exhibits pyramid-shaped islands with a lateral size of $\approx 20 \,\mathrm{nm}$ (Fig. 1(c)). The resulting layered surface is an ideal platform for acquiring spectra at a variety of Cu layer thicknesses without changing the image area. Figure 1(d) is a typical STM image of single Co adatoms on a Cu/Co/Cu(100) multilayer. Although the density of adatoms is rather high (typically 0.2 atoms/nm²), the Kondo effect remains intact as far as single adatoms appear separated from each other in an STM image.⁸

While a nominal thickness of a Cu overlayer can be estimated from the deposited amount of Cu, its local thickness varies substantially. We determined the local thickness from the energies of QW states of the Cu overlayer. 19,20,21,22,23 Since the Cu Fermi surface is lo-

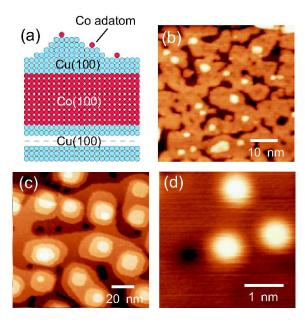


FIG. 1: (Color online) (a) Sketch of Cu/Co/Cu(100) multilayer with single adsorbed Co atoms. STM images of (b) a 10-ML-thick Co overlayer grown on a Cu(100) substrate ($I=100\,\mathrm{pA},\,V=200\,\mathrm{mV}$), (c) a 15-ML-thick Cu overlayer grown on a Co/Cu(100) multilayer ($I=100\,\mathrm{pA},\,V=200\,\mathrm{mV}$), and (d) of Co adatoms deposited on a Cu/Co/Cu(100) multilayer ($I=100\,\mathrm{pA},\,V=300\,\mathrm{mV}$).

cated near the Brillouin zone boundary, the wave function of an electronic state near the Fermi level $E_{\rm F}$ with wave number of k is modulated by an envelope function with $k_{\rm env}=k_{\rm BZ}-k$, where $k_{\rm BZ}$ is the wave number at the Brillouin zone boundary. QW states occur when electrons are reflected at the two interfaces and interfere constructively. For an electron state with $k_{\rm env}$ and energy E, this condition is satisfied when the layer thickness d_n is given by d_n

$$d_n = \left[n - 1 + \frac{\Phi(E)}{2\pi} \right] \frac{k_{\rm BZ}}{k_{\rm env}},\tag{1}$$

where $\Phi(E)$ is the total phase shift caused by the reflections and n is an integer. For E, $k_{\rm env}$ is determined by the energy dispersion of the relevant sp band (see Fig. 2(b)). Because the dispersion of the Cu sp band is precisely known near $E_{\rm F}$, the thickness of the Cu layer can be determined from the energies of the QW states.

Figure 2(a) shows a series of $\mathrm{d}I/\mathrm{d}V$ spectra taken on different surfaces of $\mathrm{Cu/Co/Cu(100)}$ multilayers. Clear peaks are visible within the range of 0 to 2.0 V indicating the presence of QW states in this energy range.²⁴ The local thickness of the Cu overlayer was determined by comparison of the experimentally obtained peak energies with calculations. The energy dispersion of the Cu sp band along the [100] direction near E_{F} can be described

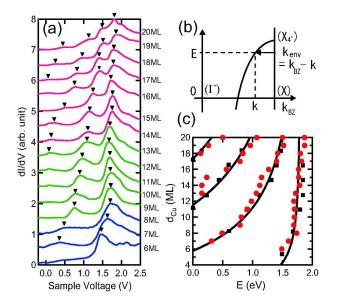


FIG. 2: (Color online) (a) Series of $\mathrm{d}I/\mathrm{d}V$ spectra measured on different surfaces of $\mathrm{Cu/Co/Cu(100)}$ multilayers. Prior to spectroscopy the tunneling gap was set at 1 nA and 2.5 V. Spectra are offset for clarity. The labels beside the graph show the thicknesses of the Cu overlayers determined by referring to theoretical curves in (c). The relative thicknesses within each group (6 – 8 ML, 9 – 13 ML, 14 – 20 ML) were determined by a simultaneously observed surface topography. (b) Schematic dispersion curve of the Cu sp band along the [100] direction $(\overline{\Gamma X})$. (c) Peak energies of $\mathrm{d}I/\mathrm{d}V$ spectra in Fig. 2(a) as a function of Cu overlayer thickness d_{Cu} (dots). Calculated energies of QW states (solid lines) and IPES data (squares)²⁰ are included.

by the two-band nearly-free electron model: ^{19,23}

$$\frac{k_{\rm env}}{k_{\rm BZ}} = \sqrt{1 + \frac{E + E_{\rm F}}{G} - \sqrt{\frac{4(E + E_{\rm F})}{G} + \left(\frac{U}{G}\right)^2}},$$
 (2)

where E is the QW state energy measured relative to the Fermi level, $G = \hbar^2 k_{\rm BZ}^2 / 2m^*$ (m^* is the effective mass of the electron), U is half the energy gap at the Brillouin zone boundary. Following the analysis of QW states observed with inverse photoemission spectroscopy (IPES) by Ortega et al., ²⁰ we insert $E_{\rm F} = 7.39 \,\mathrm{eV}$, $G = 12.27 \,\mathrm{eV}$, and $U=3.08\,\mathrm{eV}$ into Eq. (2) and a linear phase-energy relation $\Phi(E)=0.35\pi\,\mathrm{eV}^{-1}\,\times\,E$ into Eq. (1). Figure 2(c) displays the calculated thickness of a Cu overlayer as a function of QW state energies (solid lines) together with IPES data (squares).²⁰ An absolute thickness was determined for each spectrum in Fig. 2(a) by referring to these theoretical curves (see the thicknesses labeled beside the graph). Note that the relative thicknesses within a group $(6 - 8 \,\mathrm{ML}, \, 9 - 13 \,\mathrm{ML}, \, 14 - 20 \,\mathrm{ML})$ were determined by a simultaneously observed surface topography; only an identical offset was added to relative thicknesses within each group to fit all peak energies of all spectra to the theoretical curves. The results are summarized in Fig. 2(c) (dots). The excellent agreement between the ex-

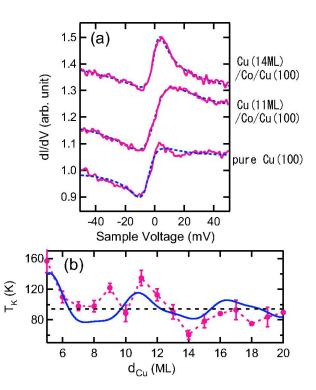


FIG. 3: (Color online) (a) $\mathrm{d}I/\mathrm{d}V$ spectra measured on Co adatoms on $\mathrm{Cu/Co/Cu(100)}$ multilayers. Top: 14 ML Cu. Middle: 11 ML Cu. Bottom: pure $\mathrm{Cu(100)}$. Spectra are offset for clarity. Dashed lines indicate fits to experimental data according to Eq. (3). (b) Averaged Kondo temperature T_{K} of Co adatoms on $\mathrm{Cu/Co/Cu(100)}$ multilayers as a function of Cu overlayer thickness d_{Cu} (circles connected by dashed line). Half the error bar represents the standard error of T_{K} calculated for each d_{Cu} . Calculated T_{K} is plotted as a solid line. The fit parameters used are $A_{\mathrm{b}} = 0.046 \, \mathrm{eV^{-1}} \, \mathrm{ML}$, $\Phi_{\mathrm{b}} = 0.26\pi$, $A_{\mathrm{n}} = 0.011 \, \mathrm{eV^{-1}} \, \mathrm{ML}$, $\Phi_{\mathrm{n}} = -0.03\pi$. Averaged $T_{\mathrm{K}} = 94 \, \mathrm{K}$ for Co adatoms on pure $\mathrm{Cu(100)}$ surfaces appears as a dotted line.

periment and the theory shows the validity of the present analysis. The thickness determination error is estimated to $\pm 1\,\mathrm{ML}$.

After determining d_{Cu} , we measured dI/dV spectra on single Co atoms on Cu/Co/Cu(100) multilayers. Before performing spectroscopy, the STM tip was shaped by touching a Cu surface area until Co adatoms appeared circular and dI/dV spectra of a bare Cu surface became featureless around zero sample voltage. For analysis of the Kondo resonance, remaining artifacts due to the tip electronic structure were removed by dividing spectra of single Co atoms by an averaged spectrum of the clean Cu surface on the same terrace. The top and middle graphs in Fig. 3(a) are representative spectra for $d_{\text{Cu}} = 14 \,\text{ML}$ and $d_{\text{Cu}} = 11 \,\text{ML}$, respectively (solid lines). As a reference, a similar measurement on a pure Cu(100) substrate is shown at the bottom of Fig. 3(a). The characteristic line shapes asymmetric around V=0 indicate the Kondo resonance on these Co adatoms. 11,14 In $\mathrm{d}I/\mathrm{d}V$ spectra the Kondo resonance generally appears as an asymmetric line shape or even as a dip due to the Fano effect. 25,26 This assignment was further confirmed by disappearance of the characteristic line shape when the tip was moved off the adatom center only by $0.5\,\mathrm{nm}.^{2,3}$

To quantitatively analyze the $\mathrm{d}I/\mathrm{d}V$ spectra, we fit the following Fano line shape to the data:^{25,26}

$$\frac{\mathrm{d}I}{\mathrm{d}V} = a\frac{(q+\epsilon)^2}{1+\epsilon^2} + b + cV \tag{3}$$

with $\epsilon = (eV - \epsilon_{\rm K})/k_{\rm B}T_{\rm K}$. Here, q is the asymmetry parameter of the Fano theory, $\epsilon_{\rm K}$ a resonance shift from the Fermi level, and a the amplitude of the resonance. A linear voltage dependence b+cV was added to account for the contribution of conduction electron states not involved in the Kondo resonance. Equation (3) was fitted to the above three spectra, with the results shown in the same graphs as dashed lines. The Kondo temperatures 67 K and 139 K were obtained for $d_{\rm Cu}=14$ ML and $d_{\rm Cu}=11$ ML, respectively, which significantly deviate from $T_{\rm K}=90$ K for pure Cu (100).²⁷

analogous performed experiments Cu/Co/Cu(100) multilayers with Cu coverages ranging between 5 and 20 ML. The total number of samples and of spectra analyzed is 10 and 156, respectively. The Fano line shape of Eq. (3) was fitted to all individual spectra to obtain $T_{\rm K}$ as described above. The whole data set was divided into groups according to d_{Cu} , and the average and the standard error of $T_{\rm K}$ were calculated for each d_{Cu} . Figure 3(b) displays the averaged T_{K} as a function of d_{Cu} (circles connected by dashed line) with half the error bar representing the standard error. Measurements on Co adatoms on pure Cu(100) were also repeated to obtain an averaged $T_{\rm K}=(94\pm5)\,{\rm K}\equiv T_{{\rm K},0}$, which is consistent with previous reports. 11,14 $T_{{\rm K},0}$ is shown as a horizontal dashed line in Fig. 3(b) as a reference.

Clearly, the Kondo temperature $T_{\rm K}$ is modulated as a function of $d_{\rm Cu}$. This $T_{\rm K}$ modulation is attributed to variations in the density of states at the Fermi level, $\rho_{\rm F}$, caused by QW states of the Cu overlayer¹⁵. The Kondo temperature depends on $\rho_{\rm F}$ through the following relation:¹

$$T_{\rm K} = T_0 \exp\left(-\frac{1}{2\rho_{\rm F}J_{\rm sd}}\right),\tag{4}$$

where T_0 is a prefactor and $J_{\rm sd}$ the s-d exchange coupling constant. This interpretation is plausible since we have proved the presence of QW states and their evolution with $d_{\rm Cu}$ in our samples. For a Co adatom on pure Cu(100), inserting $\rho_{\rm F}=0.11\,{\rm eV}^{-1},^{28}$ $J_{\rm sd}\approx 1.0\,{\rm eV},^{14,25,29}$ and $T_{\rm K,0}=94\,{\rm K}$ into Eq. (4) gives $T_0\approx 8900\,{\rm K}.$ $T_{\rm K}$ is sensitive to a small variation in $\rho_{\rm F}$ under this condition. Since the quantum confinement in the Cu/Co/Cu(100) multilayer is weak, $\rho_{\rm F}$ at the surface of the Cu overlayer is expressed by 19,21

$$\rho_{\rm F} = \rho_{\rm F,0} + \sum_{i=\rm b,n} \frac{A_i}{d_{\rm Cu}} \cos\left(\frac{2\pi d_{\rm Cu}}{\Lambda_i} + \Phi_i\right).$$
 (5)

Here, A_i , Λ_i , and Φ_i are the amplitudes, spatial periodicities, and phases of the quantum oscillations at the belly (i = b) and the neck (i = n) of the Cu Fermi surface. While the periodicities have been precisely determined $(\Lambda_{\rm b} = 5.88\,{\rm ML} \text{ and } \Lambda_{\rm n} = 2.67\,{\rm ML})^{19,21}$, the amplitudes and the phases are less established. We therefore fit $T_{\rm K}$ calculated with Eqs.(4) and (5) to the experimental data by keeping Λ_i fixed and leaving A_i and Φ_i as free parameters. The result is plotted in Fig. 3(b) (solid line) with $A_{\rm b} = 0.046 \, {\rm eV}^{-1} \, {\rm ML}, \, \Phi_{\rm b} = 0.26\pi, \, A_{\rm n} = 0.011 \, {\rm eV}^{-1} \, {\rm ML},$ and $\Phi_n = -0.03\pi$. The fit reproduces most of the aspects of the data; local maxima at ≈ 5 , ≈ 11 , and $\approx 17 \,\mathrm{ML}$ are described as well as local minima at $\approx 7-8$ and at $\approx 14 \,\mathrm{ML}$. Note that the phases determined here deviate from a theoretical prediction of $\Phi_{\rm b}=0.12\pi$ and $\Phi_{\rm n} = 0.69\pi$ for Cu/Co/Cu(100) multilayers¹⁹ by 0.14π and -0.72π , respectively. This may be attributed to additional phase shifts due to the very presence of the Co adatoms. Assuming that electron wavefunctions penetrate from the Cu surface to the vacuum side by a Co atomic height, this will result in an additional phase shift of $2\pi/\Lambda_{\rm b} = 0.34\pi$ and $2\pi/\Lambda_{\rm n} = 0.75\pi$ for $\Phi_{\rm b}$ and $\Phi_{\rm n}$, respectively. We thus call for theoretical investigations on the effect of Co adatoms on the phase shift of the quantum oscillations.

Finally, we remark that the exchange interaction between a Co adatom and the Co layer through Cu, J_{ex} , is

too weak to account for the observed variations in $T_{\rm K,0}$. According to an *ab initio* calculation by Brovko *et al.*¹⁷, $J_{\rm ex}$ is 1.5 meV for $d_{\rm Cu}=5\,{\rm ML}$ and rapidly decreases with increasing $d_{\rm Cu}$. This is small enough considering the energy scale of the Kondo effect $k_{\rm B}T_{\rm K,0}=8.1\,{\rm meV}$ observed here. However, $J_{\rm ex}$ was found to become comparable to or even much larger than $k_{\rm B}T_{\rm K,0}$ for $d_{\rm Cu}\leq 4\,{\rm ML}$. This should result in suppression and/or splitting of the Kondo resonance. ^{30,31} Furthermore, they predicted that the exchange interaction between two Co atoms adsorbed on a Cu/Co/Cu(100) multilayer can be tailored by changing the Cu overlayer thickness. ¹⁷ Our demonstration of tuning the Kondo effect by means of the same multilayer system promises experimental feasibility of such forthcoming studies.

In summary, we observed a modulation of the Kondo temperature of single Co atoms adsorbed on $\mathrm{Cu/Co/Cu(100)}$ multilayers depending on the Cu layer thickness. A model based on local density of states oscillations at the Fermi level owing to confined QW states reproduces most of the observed variations. The analysis on the T_{K} modulation suggests unexpected phases of the quantum oscillations in the Cu overlayer, which requires further experimental and theoretical efforts.

Financial support by the Deutsche Forschungsgemeinschaft through SFB 668 is acknowledged.

* Electronic address: UCHIHASHI.Takashi@nims.go.jp

A. C. Hewson, The Kondo Problem to Heavy Fermions (Cambridge University Press, Cambridge, England, 1993); K. Yoshida, Theory of Magnetism (Springer, New York, 1996).

² J. Li, W.-D. Schneider, R. Berndt, and B. Delley, Phys. Rev. Lett. **80**, 2893 (1998).

³ V. Madhavan, W. Chen, T. Jamneala, M. F. Crommie, and N. S. Wingreen, Science 280, 567 (1998).

⁴ H. C. Manoharan, C. P. Lutz, and D. M. Eigler, Nature 403, 512 (2000).

W. G. van der Wiel, S. De Franceschi, T. Fujisawa, J. M. Elzerman, S. Tarucha, and L. P. Kouwenhoven, Science 289, 2150 (2000).

⁶ J. Nygård, D. H. Cobden, and P. E. Lindelof, Nature 408, 342 (2000).

⁷ J. Park, A. N. Pasupathy, J. I. Goldsmith, C. Chang, Y. Yaish, J. R. Petta, M. Rinkoski, J. P. Sethna, H. D. Abrun, P. L. McEuen, and D. C. Ralph, Nature 417, 722 (2002); W. Liang, M. P. Shores, M. Bockrath, J. R. Long, and H. Park, Nature 417, 725 (2002).

W. Chen, T. Jamneala, V. Madhavan, and M. F. Crommie, Phys. Rev. B 60, R8529 (1999).

⁹ J. Kliewer, R. Berndt, and S. Crampin, Phys. Rev. Lett. 85, 4936 (2000).

¹⁰ L. Limot and R. Berndt, Appl. Surf. Sci. 237, 576 (2004).

¹¹ N. Néel, J. Kröger, L. Limot, K. Palotas, W. A. Hofer, and R. Berndt, Phys. Rev. Lett. 98, 016801 (2007).

A. Zhao, Q. Li, L. Chen, H. Xiang, W. Wang, S. Pan, B. Wang, X. Xiao, J. Yang, J. G. Hou, and Q. Zhu, Science

³⁰⁹, 1542 (2005).

¹³ V. Iancu, A. Deshpande, and S.-W. Hla, Phys. Rev. Lett. 97, 266603 (2006).

¹⁴ P. Wahl, P. Simon, L. Diekhöner, V. S. Stepanyuk, P. Bruno, M. A. Schneider, and K. Kern, Phys. Rev. Lett. 98, 056601 (2007).

Y.-S. Fu, S.-H. Ji, X. Chen, X.-C. Ma, R. Wu, C.-C. Wang, W.-H. Duan, X.-H. Qiu, B. Sun, P. Zhang, J.-F. Jia, and Q.-K. Xue, Phys. Rev. Lett. 99, 256601 (2007).

F. Meier, L. Zhou, J. Wiebe, and R. Wiesendanger, Science 320, 82 (2008).

¹⁷ O. O. Brovko, P. A. Ignatiev, V. S. Stepanyuk, and P. Bruno, arXiv:0804.3298.

¹⁸ T. Bernhard, R. Pfandzelter, M. Gruyters, and H. Winter Surf. Sci. **575**, 154 (2005).

¹⁹ Z. Q. Qiu and N. V. Smith, J. Phys.: Condens. Matter **14**, 169 (2002).

J. E. Ortega and F. J. Himpsel, Phys. Rev. Lett. 69, 844 (1992); J. E. Ortega, F. J. Himpsel, G. J. Mankey, and R. F. Willis, Phys. Rev. B 47, 1540 (1993).

²¹ P. Bruno, Phys. Rev. B **52**, 411 (1995); P. Bruno, J. Phys.: Condens. Matter **11** 9403 (1999).

²² P. van Gelderen, S. Crampin, and J. E. Inglesfield, Phys. Rev. B **53**, 9115 (1996).

²³ R. K. Kawakami, E. Rotenberg, E. J. Escorcia-Aparicio, H. J. Choi, T. R. Cummins, J. G. Tobin, N. V. Smith, and Z. Q. Qiu, Phys. Rev. Lett. **80**, 1754 (1998); R. K. Kawakami, E. Rotenberg, E. J. Escorcia-Aparicio, H. J. Choi, J. H. Wolfe, N. V. Smith, and Z. Q. Qiu, Phys. Rev. Lett. **82**, 4098 (1999).

- ²⁴ Peaks rather than steps are expected because only electronic states with small momenta parallel to the interface plane effectively contribute to tunneling current [see R. C. Jaklevic, J. Lambe, M. Mikkor, and W. C. Vassell, Phys. Rev. Lett. 26, 88 (1971)].
- O. Újsághy, J. Kroha, L. Szunyogh, and A. Zawadowski, Phys. Rev. Lett. 85, 2557 (2000).
- ²⁶ M. Plihal and J. W. Gadzuk, Phys. Rev. B **63**, 085404 (2001).
- We find that the Fano factor q varies significantly on Cu/Co/Cu(100) multilayers, reflecting changes in the spectrum shape. This may be caused by quantum interference

- in the Cu overlayer. $^{26}\,$
- $\rho_{\rm F}$ was estimated within the free electron model.
- P. Wahl, L. Diekhöner, M. A. Schneider, L. Vitali, G. Wittich, and K. Kern, Phys. Rev. Lett. 93, 176603 (2004).
- A. N. Pasupathy, R. C. Bialczak, J. Martinek, J. E. Grose, L. A. K. Donev, P. L. McEuen, D. C. Ralph, Science 306, 86 (2004).
- J. Martinek, M. Sindel, L. Borda, J. Barnaś, J. König, G. Schön, and J. von Delft, Phys. Rev. Lett. 91, 247202 (2003).